ACS APPLIED MATERIALS & INTERFACES

Biological and Medical Applications of Materials and Interfaces

Organic Electrochemical Transistors for the Detection of Cell Surface Glycans

Lizhen Chen, Ying Fu, Naixiang Wang, Anneng Yang, Yuanzhe Li, Jie Wu, Huangxian Ju, and Feng Yan

ACS Appl. Mater. Interfaces, **Just Accepted Manuscript** • DOI: 10.1021/acsami.8b01987 • Publication Date (Web): 11 May 2018

ACS Publications

is published by the American Chemical Society. 1155 Sixteenth Street N.W., Washington, DC 20036

Organic Electrochemical Transistors for the Detection of Cell Surface Glycans

Lizhen Chen,[†,‡,§] Ying Fu,[‡,§] Naixiang Wang,[‡] Anneng Yang,[‡] Yuanzhe Li,[‡] Jie Wu,[†] Huangxian Ju,[†,*] and Feng Yan[‡,*]

[†] *State Key Laboratory of Analytical Chemistry for Life Science, School of Chemistry and Chemical Engineering, Nanjing University, Nanjing 210023, China*

[‡] *Department of Applied Physics, The Hong Kong Polytechnic University, Hong Kong*

KEYWORDS: Organic electrochemical transistor; Glycan; Cancer cell; Aptamer; Nanoprobe

* Corresponding authors: hxju@nju.edu.cn (H. Ju) and apafyan@polyu.edu.hk (F. Yan)

ABSTRACT: Cell surface glycans play critical roles in diverse biological processes, such as cell-cell communication, immunity, infection, development and differentiation. Their expressions are closely related to cancer growth and metastasis. This work demonstrates an organic electrochemical transistor (OECT)-based biosensor for the detection of glycan expression on living cancer cells. Herein, mannose on human breast cancer cells (MCF-7) as target glycan model, poly dimethyl diallyl ammonium chloride-multiwall carbon nanotubes (PDDA-MWCNT) as loading interface, concanavalin A (Con A) with active mannose binding sites, aptamer- and horseradish peroxidase co-immobilized gold nanoparticles (HRP-aptamer-Au NPs) as specific nanoprobes are used to fabricate the OECT biosensor. In this strategy, PDDA-MWCNT interfaces can enhance the loading of Con A, and the target cells can be captured through Con A via active mannose binding sites. So the expression of cell surface can be reflected by the amount of cells captured on the gate. Specific nanoprobes are introduced to the captured cells to produce an OECT signal due to the reduction of hydrogen peroxide catalyzed by horseradish peroxidase conjugated on Au nanoparticles, while the aptamer on nanoprobes can selectively recognize the MCF-7 cells. It's reasonable that more target cells are captured on the gate electrode, more HRP-nanoprobes are loaded thus a larger signal response. The device shows an obvious response to MCF-7 cells down to 10 cells/μL, and can be used to selectively monitor the change of mannose expression on cell surfaces upon a treatment with N-glycan inhibitor. The OECT-based biosensor is promising for the analysis of glycan expressions on the surfaces of different types of cells.

1. INTRODUCTION

Glycoproteins, which are widely found in eukaryotic cells, play the roles of cellular or molecular biological identification in biological processes. Carbohydrate in glycoproteins on a cell surface is involved in most physiological processes, including proliferation, differentiation, growth, information transmission, death and progression of cancer.[1-6] Variable glycosylation on cell surface also plays important roles in biological processes. Generally, the main configurations of sugar chains in glycoproteins are N-glycans and O-glycans. The special characteristic of N-glycans is the core structure of pentasaccharide,[7] which represents the majority of protein glycosylation. As a result, the dynamic monitoring of N-glycan on a cell surface gives a new insight into clinical diagnoses. Many methods have been developed to realize dynamic analysis of cell glycans, such as high-performance liquid chromatography (HPLC),[8] mass spectrometry (MS),[9] nuclear magnetic resonance (NMR),[10] Raman spectrum,[11] fluorescence[12] and electrochemistry.[13-15] Although being successfully used, these methods have some drawbacks for living cell analysis. For example, glycans, usually chemical labelled, must be enzymatic cleave from living cells as its complex microenvironment to give an exact signal in HPLC, MS and NMR spectrum. Therefore, it is necessary to develop a highly sensitive approach to detect the glycan expression on cell surfaces based on non-destructive, low-cost and convenient procedures.

Organic bioelectronics has attracted much attention recently for its promising applications in various biological sensing.[16-19] Organic electronic devices that can monitor biological signals will play an important role in understanding biological processes in real physical environment. In particular, organic electrochemical transistors (OECTs) have demonstrated the great potential in biological sensing owning to the high sensitivity of the devices, and have shown many other advantages, including low cost, flexibility, easy fabrication and low working voltage (<1 V).[20-26]

They have been successfully applied in the detection of some small molecules, such as dopamine,[27] glucose,[28] epinephrine,[29] gallic acid[30] and alcohols,[31] as well as many macromolecules, including DNA,[32] protein,[33-34] bacteria[35] and cells.[36] However, highly sensitive glycan sensors based on OECTs have never been reported.

In this paper, we present an OECT-based biosensor for the detection of a glycan on a cell surface. The device contains an organic channel based on poly(3,4-ethylenedioxythiophene): poly(styrene sulfonic acid) (PEDOT:PSS) and a gate electrode modified with concanavalin A (Con A) loaded by PDDA-MWCNT that can specifically bind mannose and capture cancer cells. Specific nanoprobes prepared by co-immobilizing horseradish peroxidase (HRP) and aptamer on gold nanoparticles (HRP-aptamer-Au NPs) are then used to specifically modify human breast cancer (MCF-7) cells, which enables the gate electrode to be electrochemically active. Therefore, the designed OECT-based glycan biosensor gives direct current signals with the cells loaded on the gate electrode and the amount of mannose on cell surfaces can influence the number of captured cells and thus the device performance. The sensors show obvious current responses to MCF-7 cells through the HRP-catalyzed reduction of hydrogen peroxide even when the cell concentration is as low as 10 cells/μL, and the signal is dramatically decreased upon N-glycan inhibitor stimulation due to the decrease of mannose expression on cells. Moreover, the devices can be used in the analysis of other glycans and cancer cells by changing the binding lectin and the aptamer sequence. The work indicates that the OECT-based glycan biosensor can be developed as a promising technique for biological analysis and the diagnosis of related diseases.

2. EXPERIMENTAL SECTION

2.1. Reagents and Materials. Multi-wall carbon nanotubes (MWCNT) was supplied by Nanjing XFNANO Materials Tech Co. Ltd.. Poly dimethyl diallyl ammonium chloride (PDDA, Mw = 20000

~ 35000), $HAuCl_4 \cdot 4H_2O$, citrate sodium, NaCl, Na_2CO_3, tris (2-carboxyethyl) phosphine (TCEP), horseradish peroxidase (HRP), concanavalin A (Con A), bovine serum albumin (BSA), tunicamycin (TM) and benzyl 2-acetamido-2-deoxy-α-D-galactopyranoside (BG) were purchased from Sigma-Aldrich, USA. To prepare OECTs, acetone, isopropanol (IPA), dimethylsulfoxide (DMSO) and glycerin with ACS grade were used. Poly (3,4-ethylenedioxythiophene) doped with poly (styrene sulfonate) (PEDOT:PSS, Clevios^{TM}, PH 500) was bought from Heraeus, Germany. Phosphate buffered saline (PBS), tris (hydroxymethyl) aminomethane (Tris-HCl), cell culture medium (Dulbecco's modified eagle medium, DMEM) and fetal bovine serum were bought from Thermo Fisher Scientific Inc. The aptamer to MCF-7 cells was obtained from Shanghai Sangon Biological Engineering Technology & Services Co. Ltd.. Its sequence was 5′-GCAGTTGATCCTTTGGATACCCTGGTTTTTTTTTT-SH-C_6H_{12}-3′.

2.2. Characterization and Apparatus. The three electrodes of an OECT were connected to two Keithley source meters (Keithley 2400) and measured under different gate voltages. The output signals were recorded and saved by the customized Labview software. Shimadzu 2550 was applied for UV-Vis characterization of Au NPs. Transmission electron microscope (TEM) and high-resolution TEM (HRTEM) (JEOL-2100F) and scanning electron microscope (SEM) (JEOL Model JSM-6490) were used to characterize the nanomaterials and the biological modification. The Zeta potential was obtained by the 90 Plus DynaPro nanostar (Brookhaven Instrument Corporation，USA). The optical images were obtained under a Nikon Eilipse 80i microscope.

2.3. Preparation of PDDA-MWCNT. MWCNT sample was first treated with the mixture of HNO_3/H_2SO_4 (1:3 v/v). The mixed dispersion was sonicated for 4 h, followed by centrifugation at

13000 rpm and washing with water till the pH was neutral. The procedure generated carboxylate groups on the surface of MWCNT. PDDA was used to change the charge state on carbon nanotubes. 0.5 mg/mL of carboxylated MWCNT dispersion was mixed with 0.2% wt PDDA solution in ultrasound for 30 min. Excess PDDA was removed by centrifugation at 13000 rpm, and the complex was washed with water to obtain PDDA-functionalized MWCNT (named PDCNT).

2.4. Synthesis of Au Nanoprobe. Au nanoparticles (Au NPs) were synthesized in one-pot method.[37] Briefly, 3 mL of 1% wt trisodium citrate solution was quickly added into the 100 mL of boiling 0.01% wt $HAuCl_4$ solution with stirring. The solution turned red when Au NPs were formed, then the solution was stopped heating and left stirring to cool down. The Au NPs solution was stored at 4°C for future use.

DNA aptamer (50 μM) was activated by 1mM TCEP in 50 mM Tris-HCl buffer (pH 7.4) for 1 h at room temperature before conjugating with gold nanoparticle. 5 mL of Au NPs colloids solution was adjusted to pH 9.0 by 0.1 M Na_2CO_3, then 50 μL of HRP solution (1mg/mL) was added and kept stirring for 3 h at room temperature. 70 μL of aptamer was added into solution and kept for 24 h at 4°C. After incubation, 100 μL of 1 M NaCl was added to age the aptamer, the resulting solution was placed at 4°C for another 24 h.

2.5. Cell Culture and Treatment. All cell lines were obtained from ATCC. Cells were cultured in a DMEM medium containing 10% fetal bovine serum at 37°C with 5% CO_2 for proliferation. The cultured cells were washed with PBS to remove the culture medium at 1000 rpm and counted to obtain the certain concentration of PBS dispersion. To stimulate the glycan expression on cell surface, MCF-7 cells were treated with the inhibitors of N-glycan expression (TM) and O-glycan

expression (BG), respectively. In detail, TM- and BG-treated MCF-7 cells were obtained by incubating cells in the cell culture medium with 1000 cells/μL containing different concentrations of TM and BG for 48 h, respectively.

2.6. Biosensor Fabrication. The OECT devices were fabricated on glass substrates (Figure 1A). The size of the glass substrate was 1.1 cm ×1.2 cm. Cr/Au drain/source/gate electrodes were deposited on the glass substrate by magnetron sputtering through a shadow mask. The channel width and length of the device were 0.2 mm and 6 mm, respectively, while the area of the Au gate electrode was 3 mm × 3 mm. After the substrate was washed with acetone and treated with oxygen plasma, PEDOT:PSS with 5% v/v glycerin and 5% v/v DMSO was spin-coated on the substrate to form an organic channel between source and drain electrodes. The devices were annealed at 130 °C for 1 h in a glovebox filled with high-purity N_2. The bare Au gate electrode was then dropped with 5 μL of PDCNT dispersion to form a thin layer at room temperature. 10 μL Con A solution (1 mg/mL) was finally dropped on the PDCNT layer and to incubate for 1 h, followed by 10 μL of 0.1% BSA solution to block the nonspecific binding sites for another 1 h to BSA/Con A/PDCNT/Au gate electrode as the OECT-based biosensor.

2.7. Cell Surface Mannose Detection. After the biosensors were incubated with 10 μL of different concentrations of cells for 1 h, the cells were captured via the specific binding between Con A and surface mannose. 10 μL of nanoprobe solution was then dropped on the biosensor to incubate for another 1 h, which introduced the nanoprobe to captured cells via the strong affinity between aptamer and cell surface. After rinsing with PBS, the Au nanoprobe/cell/BSA/Con A/PDCNT/Au gate electrode was obtained for detection of cell surface mannose by immersing it into 10 mL PBS

electrolyte. The drain voltage was fixed at 0.05 V, and the V_g was set at 0.9 V in the I_d-time tests. 100 μM H_2O_2 was quickly added into the PBS when the drain current reached steady.

3. RESULTS AND DISCUSSION

3.1. Design of OECT-based Mannose Biosensor. In this work, we used mannose (inset, Figure 1A) as a target glycan. Mannose is one of the building blocks of all mammalian glycans and is the core fragment of N-glycans on the cell surface.[38-39] So, it is necessary to evaluate its expression on cancer cell surface. However, mannose is not electrochemically active and its interactions with an organic semiconductor can be very weak, which makes it difficult to be directly detected by OECTs. Unlike glucose that has glucose oxidase enzyme to induce peroxidase reaction for an electrochemical signal, mannose doesn't have such oxidase enzyme. On the other hand, because of its simple structure, mannose cannot bind with two selective receptors and be tested by using a sandwiched type biosensor that was reported in our previous work.[33] Therefore, it is a challenge to detect N-glycan with an OECT.

Figure 1A shows the design of the gate electrode of an OECT. The Au gate electrode is modified with PDCNT, Con A and BSA, sequentially, by solution processes. PDCNT was utilized to enhance the loading amount of Con A on the electrode due to large recognition interfaces of carbon nanotubes. Con A with an isoelectric point of around 5 was negatively charged in PBS with pH 7.0. As PDCNT was positively charged, Con A could be conveniently adsorbed on the surface of PDCNT due to an electrostatic interaction. The extra active sites are then blocked with BSA to avoid nonspecific absorption on PDCNT.[40] The Con A adsorbed on the gate electrode can selectively bind mannose site in cell surface glycans.

The capture of MCF-7 cancer cells is performed by incubating different concentrations of cells on Con A adsorbed biosensor surfaces. The number of captured cells is dependent on the amount of cell surface mannose, thus the treatment of MCF-7 cancer cells with N-glycan inhibitor tunicamycin (TM)[41] can decrease the number of captured cells (Figure 1B). Then nanoprobes are introduced on the surface of captured cells due to the specific binding of the aptamer on the nanoprobes to the cell surface,[42] leading to an electrochemically active gate electrode. The OECT is then characterized in PBS solution with an addition of hydrogen peroxide (H_2O_2) of 100 μM (Figure 1C). The reduction of H_2O_2 catalyzed by HRP immobilized on the nanoprobes can lead to a change of the effective gate voltage (V_g^{eff}) and consequently a change of the channel current of the OECT. Therefore, mannose expression on cancer cell surface can be analyzed.

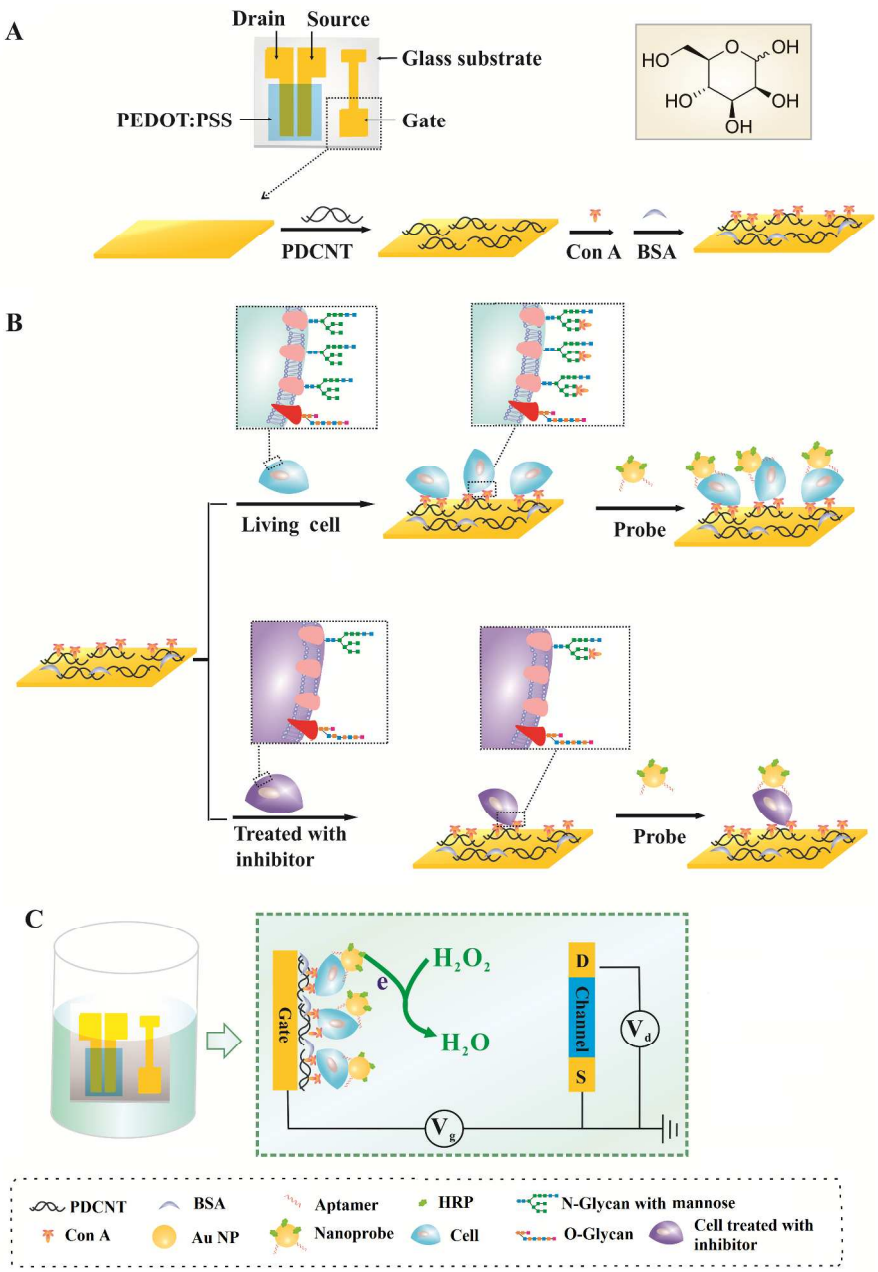

Figure 1. Biofunctionalization of OECTs for glycan sensing. (A) Schematic illustration of general device design. Inset: chemical structure of mannose. (B) Schematic for gate modification procedure with Con A to capture mannose on cell surface and recognition of nanoprobe to captured cancer cells. (C) Schematic of OECT-based biosensor and the electrochemical reaction at the gate electrode in PBS solution.

3.2. Characterization of Nanoprobes and PDCNT. Au NPs were synthesized using a typical one-pot method, which showed an average size of about 13 nm (Figure 2A). Clear lattice fringe of gold planes can be observed under HRTEM (Figure S1A),[43] indicating the successful fabrication of Au NPs. The UV-vis spectrum of bare Au NPs showed an obvious absorption peak around 520 nm, while nanoprobes showed an absorption peak near 530 nm. The conjugation of HRP and aptamer on the surface of Au NPs increased the localized refractive index, thus a visible red-shifted peak could be distinguished in the spectrum (Figure 2B).[44-45] As mentioned before, PDDA was introduced to change the charge state of carboxylated carbon nanotubes(COOH-MWCNT). The Zeta potential was changed from -31.64 mV to 12.88 mV after PDDA was wrapped on the nanotube, which confirmed the PDCNT being positively charged (Figure S1B). After PDCNT was coated on a gate electrode, the film was observed to have a well-dispersed structure under SEM (Figure 2C), which could provide a good micro-environment for biomolecule loading. The loading of Con A and BSA on PDCNT modified gate electrode greatly changed its surface morphology (Figure 2D), and the film became thicker, indicating effective immobilization of Con A on the gate electrode.

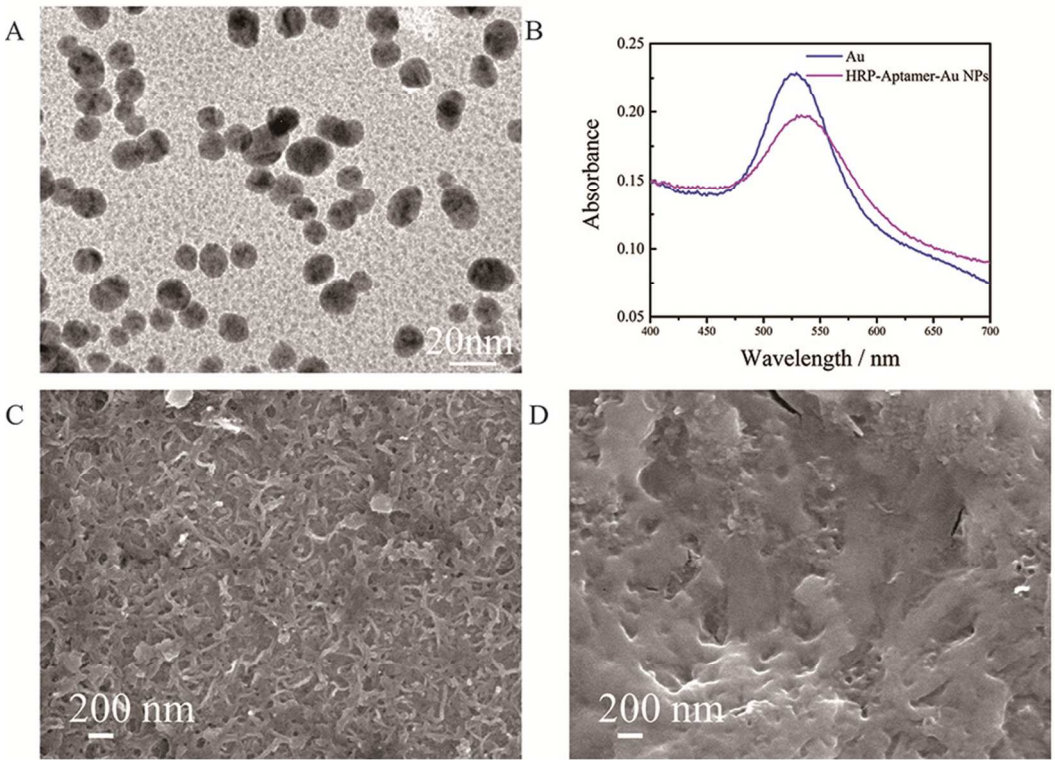

Figure 2. (A) TEM image of Au NPs. (B) UV-vis spectra of bare Au NPs and nanoprobe. SEM images of (C) PDCNT and (D) BSA@Con A modified gate electrodes.

3.3. Transistor Performance of OECT-based Biosensor. The transfer curve of an OECT with a Con A-modified gate electrode in PBS solution showed the channel current change of one order of magnitude under the gate voltages varied from 0 to 1.2 V (Figure 3A). The transconductance (g_m) reached the maximum value of 0.4 mS at V_g of around 0.9 V, suggesting good transistor performance even after the modification of Con A. V_g = 0.9 V was selected as the operation condition for the following measurements due to the maximum transconductance. After loading living MCF-7 cancer cells (1000 cells/μL) on Con A-modified gate electrodes of OECTs, this device showed very low response to 100 μM H_2O_2 at V_{ds} of 0.05 V and V_g of 0.9 V, and 1-hour incubation of the cell loaded device with PBS did not change the background (Figure 3B). However, 1-hour incubation of the cell

loaded device with nanoprobes led to an obvious response to 100 μM H_2O_2, indicating that the nanoprobes could effectively recognize the living MCF-7 cancer cells to catalyze H_2O_2 reduction.

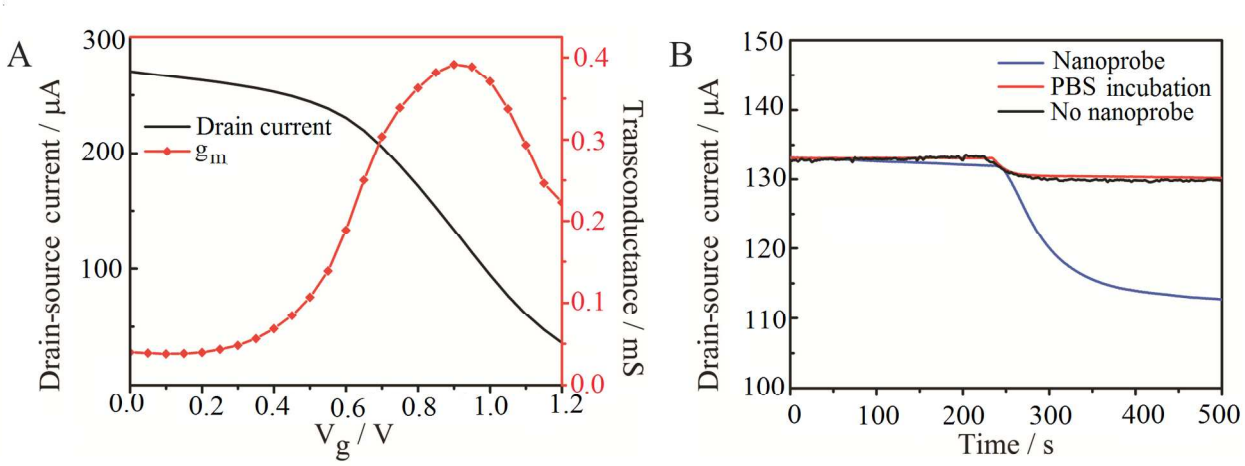

Figure 3. (A) Transfer curve and transconductance (g_m) of Con A -modified OECT biosensor in PBS at V_{ds} of 0.05 V. (B) I_d-time curves of Au nanoprobe/cell/BSA/Con A/PDCNT/Au gate electrode and cell/BSA/Con A/PDCNT/Au gate electrode with and without PBS incubation for 1 h in PBS upon addition of 100 μM H_2O_2 at V_{ds} of 0.05 V and V_g of 0.9 V.

3.4. Cancer Cell Detection with OECTs. According to the device design, OECTs were ready for mannose analysis on living MCF-7 cancer cells by recording channel currents of Au nanoprobe/cell/BSA/Con A/PDCNT/Au gate electrodes as a function of time (I_d-time) at the V_{ds} of 0.05 V and V_g of 0.9 V in PBS upon addition of 100 μM H_2O_2. As shown in Figure 4A, the current response increased with the increase of MCF-7 concentration, indicating that more cells were attached to the gate electrode. The current response is due to the change of the effective gate voltage (ΔV_g^{eff}) of the transistor. The ΔV_g^{eff} could be calculated from the channel current change and the

transfer curve, and fitted with the following equation, which was similar to other types of OECT-based biosensors:[21]

$$\Delta V_g^{eff} \propto \alpha Log[N_{cell}], \quad (1)$$

where α is a constant. The least square fitting (dash line) showed the α value of 11.37 mV/decade (Figure 4B). Notably, the device showed similar responses towards the concentration of 10^4 cell/μL and 10^5 cell/μL, indicating that the device reached saturation. So the concentration over 10^4 cell/μL was out of the linear range. The device could detect cell concentration down to 10 cells/μL.

To obtain the best performance, the amount of nanoprobes used in the experiments was optimized. The optimum condition was found to be 10 μL. Further increase of nanoprobe volume could not enhance the response (Figure 4C). We also tested other types of cells (MDA-MB 231, MCF-10A and H9C2) by using same OECTs to show the device selectivity. MDA-MB 231 cells are ER-negative breast cancer cells. MCF-10A cells are normal mammalian cells and H9C2 cells are another kind of normal cells. Compared to MDA-MB 231, MCF-10A and H9C2 cells, MCF-7 cancer cells as one kind of ER-positive cancer cells showed a much greater response due to the binding of nanoprobes on their surfaces via aptamer (Figure 4D).[41] Therefore, the OECT biosensor showed good selectivity to mannose expressed cells, which is of great importance in the analysis of some special cells.

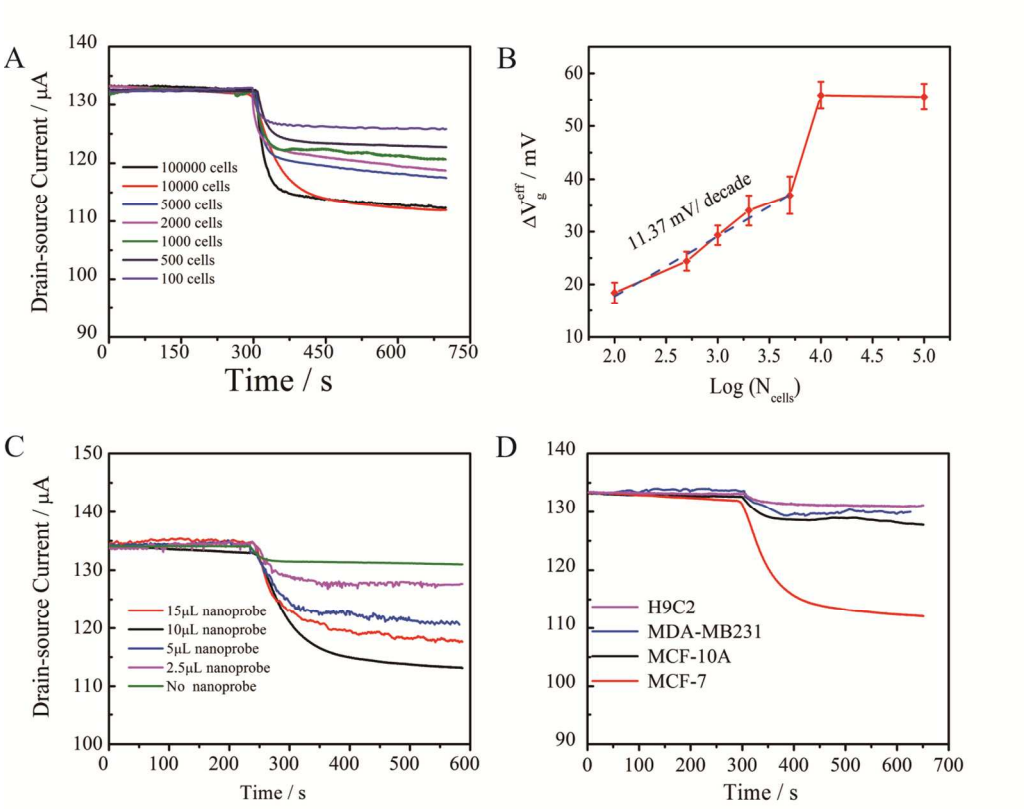

Figure 4. (A) I_{DS}-time curves of OECT biosensor at different concentrations of MCF-7 cells upon addition of 100 μM H_2O_2 at V_{ds} of 0.05 V and V_g of 0.9 V. (B) Plot of ΔV_g^{eff} *vs* log(N_{cells}). Dash line corresponds to the fitting of the data by equation (1) for cell concentrations lower than 10^4 cell/μL. (C) Current change towards nanoprobe volume for measurements of I_{DS}-time curves. (D) Selectivity of OECT biosensor towards different cells. Cell concentration in (C) and (D) was 1000 cells/μL.

3.5. Mannose Expression on Cell Surface upon Inhibitor Treatment. The OECT biosensors were used to detect the change of mannose expression on cell surface upon treatment with N-glycan inhibitor. TM is an N-glycan inhibitor that can block the first step in the biosynthesis of N-glycosylation in cells, which greatly affects the expression of mannose on cell surface. At the MCF-7 cells concentration of 1000 cells/μL, these cells were firstly treated with 0.05 to 10 μg/mL TM for 48

h, and then purified by centrifuging at 1000 rpm for 5 min. Notably, the current response decreased with the increasing TM concentration from 0.05 μg/mL to 5 μg/mL (Figure 5A), which led to lower mannose expression on cancer cells. When the TM concentration reached 10 μg/mL, the current response showed little change owing to the saturated inhibition effect of TM. This result was similar to the cases for many other inhibitors previously studied, and the half-maximal inhibition value was estimated to be around 0.08 μg/mL (Figure 5B).[46] We can find that the error bars calculated from 3 parallel modified sensors shown in Figure 5B are rather short, which also show high reliability and stability of the devices. The results are consistent with our previous works of OECT-based biosensors.[47-50]

To explore the binding specificity of Con A and mannose, an O-glycan inhibitor, benzyl 2-acetamido-2-deoxy-α-D-galactopyranoside (BG), was used to treat the cells. After MCF-7 cells were treated with 50 μg/mL BG for 48 h, the current response did not show significant change in comparison with untreated or solvent DMSO treated MCF-7 cells (Figure 5C), indicating high mannose expression on BG-treated cells and that solvent DMSO did not influence the measurement. With the increasing treatment time with TM, the current response decreased (Figure 5D), indicating the continuous decrease of mannose expression on the cell surface. Thus the OECT biosensors could be used to monitor the change of mannose expression on a cell surface.

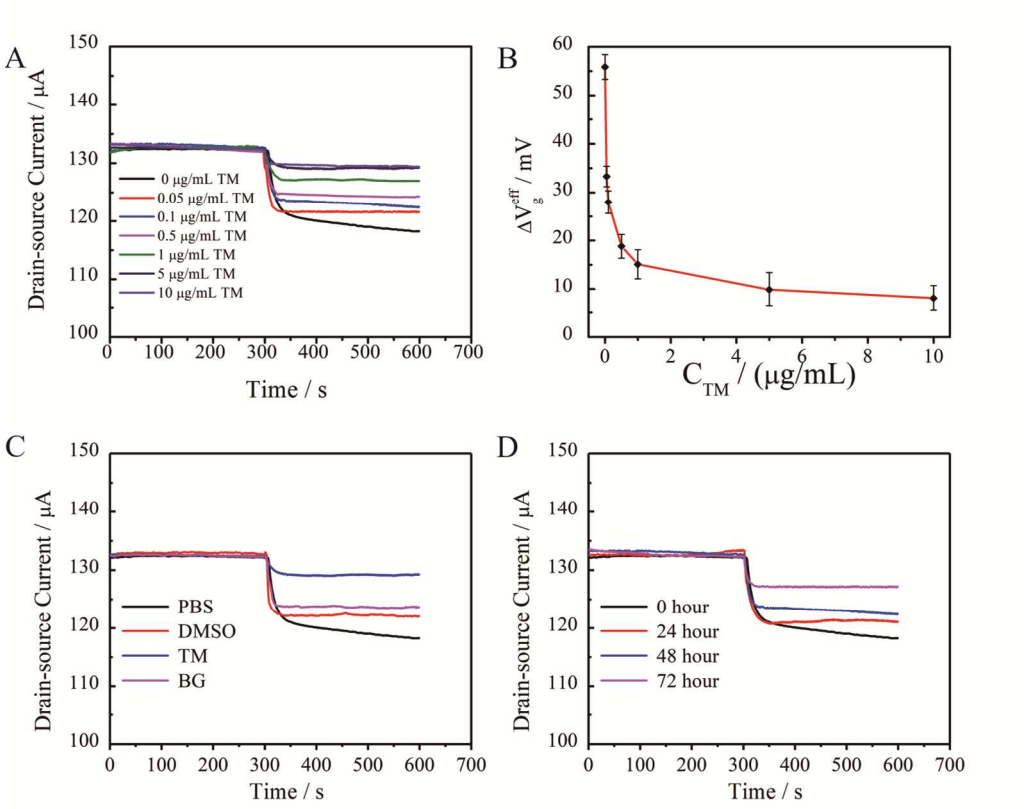

Figure 5. Current responses to MCF-7 cells **(**A) treated with different concentrations of TM, **(**B) Plot of ΔV_g^{eff} *vs* different concentrations of TM. The error bar was calculated from 3 parallel modified sensors. (C) untreated or treated with DMSO, 0.05 μg/mL TM or 50 μg/mL BG in DMSO for 48 h, and (D) treated with 0.1 μg/mL TM for different times.

3.6. Optical Monitoring of Cells Captured on Gate Electrodes. The binding of Con A to MCF-7 cells was finally confirmed by fluorescence imaging. Living MCF-7 cells were stained with green fluorescence dye (SYTO green fluorescent nucleic acid stain from Thermo Fisher Co.) at 37 ºC for 15 min and washed with PBS for three times. After the stained cells were incubated on the gate electrode for 1 h, the electrode showed the fluorescence of SYTO green, while bare Au electrode did not show obvious fluorescence (Figure 6A and 6B). Moreover, the fluorescence intensity increased with the increased concentration of SYTO green-stained MCF-7 cells (Figure 6B and 6C), indicating

more cells were captured on the gate electrode. It was reasonable to conclude that the amount of cells captured on the gate electrode increased with the increase of cell concentration.

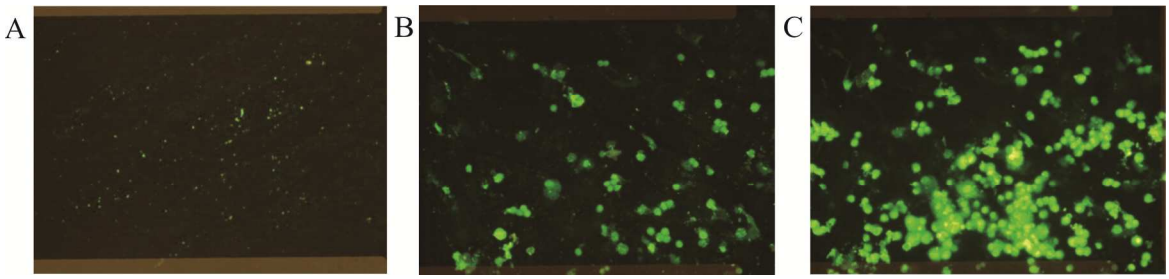

Figure 6. Fluorescence images of (A) gate electrode and (B) BSA/Con A/PDCNT modified gate electrode incubated with 100 cells/μL SYTO green-stained MCF-7 cells for 1 h, and (C) BSA/Con A/PDCNT modified gate incubated with 1000 cells/μL SYTO green-stained MCF-7 cells for 1 h.

4. CONCLUSIONS

In summary, we successfully used OECTs for the analysis of mannose expression on living cancer cells based on the interaction between Con A immobilized on the gate electrode and mannose sites on the cell surfaces. The devices were used to selectively detect cancer cells with a concentration down to 10 cells/μL due to the high expression of mannose on the cell surface. More importantly, the change of mannose expression on cell surfaces upon the treatment of glycan inhibitors were successfully monitored. This strategy provides a convenient and versatile sensing platform for the analysis of various glycans on a cell surface.

■ AUTHOR INFORMATION

Corresponding Author

*E-mail: hxju@nju.edu.cn.

* E-mail: apafyan@polyu.edu.hk.

ORCID

Huangxian Ju: 0000-0002-6741-5302

Feng Yan: 0000-0001-7385-6334

Author Contributions

[§] Lizhen Chen and Ying Fu contributed equally to this work.

Notes

The authors declare no competing financial interests.

■ ACKNOWLEDGMENT

This work was financially supported by the Research Grants Council (RGC) of Hong Kong, China (Project No. N_PolyU506/13), the Hong Kong Polytechnic University (Project No. G-SB51, 1-YW0Y), and the National Natural Science Foundation of China (21361162002, 21635005).

■ REFERENCES

(1) Dennis, J. W.; Nabi, I. R.; Demetriou M. Metabolism, Cell Surface Organization, and Disease. *Cell* **2009**, *139*, 1229-1241.

(2) Flanagan-Steet, H. R.; Steet, R. "Casting" Light on the Role of Glycosylation during Embryonic Development: Insights from Zebrafish. *Glycoconj. J.* **2013**, *30*, 33-40.

(3) Gu, J. G.; Isaji, T.; Xu, Q. S.; Kariya, Y.; Gu, W.; Fukuda, T.; Du, Y. G. Potential Roles of N-Glycosylation in Cell Adhesion. *Glycoconj. J.* **2012**, *29*, 599-607.

(4) Haltiwanger, R. S.; Lowe, J. B. Role of Glycosylation in Development. *Annu. Rev. Biochem.* **2004**, *73*, 491-537.

(5) Lau, K. S.; Dennis, J. W. N-Glycans in Cancer Progression. *Glycobiology* **2008**, *18*, 750-760.

(6) Marth, J. D.; Grewal, P. K. Mammalian Glycosylation in Immunity. *Nat. Rev. Immunol*. **2008**, *8*, 874-887.

(7) Marino, K.; Bones, J.; Kattla, J. J.; Rudd, P. M. A Systematic Approach to Protein Glycosylation Analysis: A Path through the Maze. *Nat. Chem. Biol.* **2010**, *6*, 713-723.

(8) Royle, L.; Campbell, M. P.; Radcliffe, C. M.; White, D. M.; Harvey, D. J.; Abrahams, J. L.; Kim, Y. G.; Henry, G. W.; Shadick, N. A.; Weinblatt, M. E.; Lee, D. M.; Rudd, P. M.; Dwek, R. A. HPLC-Based Analysis of Serum N-Glycans on a 96-Well Plate Platform with Dedicated Database Software. *Anal. Biochem.* **2008**, *376*, 1-12.

(9) Nishikaze, T.; Kaneshiro, K.; Kawabata, S.; Tanaka, K. Structural Analysis of N-Glycans by the Glycan-Labeling Method Using 3-Aminoquinoline-Based Liquid Matrix in Negative-Ion MALDI-MS. *Anal.Chem.* **2012**, *84*, 9453-9461.

(10) Carneiro, M. G.; Koharudin, L. M. I.; Ban, D.; Sabo, T. M.; Trigo-Mourino, P.; Mazur, A.; Griesinger, C.; Gronenborn, A. M.; Lee, D. Sampling of Glycan‐Bound Conformers by the Anti‐

HIV Lectin Oscillatoria agardhii agglutinin in the Absence of Sugar. *Angew. Chem., Int. Ed.* **2015**, *54*, 6462-6465.

(11) Chen, Y. L.; Ding, L.; Xu, J. Q.; Song, W. Y.; Yang, M.; Hu, J. J.; Ju, H. X. Micro-Competition System for Raman Quantification of Multiple Glycans on Intact Cell Surface. *Chem. Sci.* **2015**, *6*, 3769-3774.

(12) Fu, Y.; Lu, D. Q; Lin, B.; Sun, Q. Q; Liu, K.; Xu, L. L.; Zhang, W. Fluorescence Assay for Glycan Expression on Living Cancer Cells Based on Competitive Strategy Coupled with Dual-Functionalized Nanobiocomposites. *Analyst* **2013**, *138*, 7016-7022.

(13) Chen, X. J.; Wang, Y. Z.; Zhang, Y. Y.; Chen, Z. H.; Liu, Y.; Li, Z. L.; Li, J. H. Sensitive Electrochemical Aptamer Biosensor for Dynamic Cell Surface N-Glycan Evaluation Featuring Multivalent Recognition and Signal Amplification on a Dendrimer–Graphene Electrode Interface. *Anal. Chem.* **2014**, *86*, 4278-4286.

(14) Zhang, X. A.; Teng, Y. Q.; Fu, Y., Xu, L. L.; Zhang, S. P.; He, B.; Zhang, W. Lectin-Based Biosensor Strategy for Electrochemical Assay of Glycan Expression on Living Cancer Cells. *Anal. Chem.* **2010**. *82*, 9455-9460.

(15) Cheng, W.; Ding, L.; Ding, S. J.; Yin, Y. B.; Ju, H. X. A Simple Electrochemical Cytosensor Array for Dynamic Analysis of Carcinoma Cell Surface Glycans. *Angew. Chem. Int. Ed.* **2009**, *48*, 6465-6468.

(16) Wang, N. X.; Liu, Y. Z.; Fu, Y.; Yan, F. AC Measurements Using Organic Electrochemical Transistors for Accurate Sensing. *ACS Appl. Mater. Interfaces* **2018,** DOI: 10.1021/acsami.7b07668.

(17) Tarabella, G.; Santato, C.; Yang, S. Y.; Iannotta, S.; Malliaras, G. G.; Cicoira, F. Effect of the Gate Electrode on the Response of Organic Electrochemical Transistors. *Appl. Phys. Lett*. **2010**, *97*, 123304.

(18) Liao C. Z.; Zhang, M.; Yao, M. Y.; Hua, T.; Li, L.; Yan, F. Flexible Organic Electronics in Biology: Materials and Devices, *Adv. Mater*. **2015**, *27*, 7493-7527.

(19) Roberts, M. E.; Mannsfeld, S. C.; Queraltó, N.; Reese; C.; Locklin, J.; Knoll, W.; Bao, Z. N. Water-Stable Organic Transistors and Their Application in Chemical and Biological Sensors. *Proc. Natl. Acad. Sci. U S A*, **2008**, *105*, 12134-12139.

(20) Lin, P.; Yan, F. Organic Thin Film Transistors for Chemical and Biological Sensing, *Adv. Mater.* **2012**, *24*, 34-51.

(21) Rivnay, J.; Inal, S.; Salleo, A.; Owens, R. M.; Berggren, M.; Malliaras, G. G. Organic Electrochemical Transistors. *Nat. Rev. Mater.* **2018**, *3*, 17086.

(22) Kergoat, L.; Piro, B.; Simon, D. T.; Pham, M. C.; Noël, V.; Berggren, M. Detection of Glutamate and Acetylcholine with Organic Electrochemical Transistors Based on Conducting Polymer/Platinum Nanoparticle Composites. *Adv. Mater.* **2014**, *26*, 5658-5664.

(23) Khodagholy, D.; Rivnay, J.; Sessolo, M.; Gurfinkel, M.; Leleux, P.; Jimison, L. H.; Malliaras, G. G. High Transconductance Organic Electrochemical Transistors. *Nat. commun.* **2013**, *4*. 2133.

(24) Bernards, D. A.; Malliaras, G. G. Steady-State and Transient Behavior of Organic Electrochemical Transistors. *Adv. Funct. Mater.* **2007**, *17*, 3538-3544.

(25) Zhang, S. M.; Hubis, E.; Tomasello, G.; Soliveri, G.; Kumar, P.; Cicoira, F. Patterning of Stretchable Organic Electrochemical Transistors. *Chem. Mater.* **2017**, *29*, 3126-3132.

(26) Zhang, S. M.; Hubis, E.; Girard, C.; Kumar, P.; DeFranco, J.; Cicoira, F. Water stability and Orthogonal Patterning of Flexible Micro-electrochemical Transistors on Plastic. *J. Chem. Mater.* C, **2016**, *4*, 1382-1385.

(27) Tang, H.; Lin, P.; Chan, H. L.; Yan, F. Highly Sensitive Dopamine Biosensors Based on Organic Electrochemical Transistors. *Biosens. Bioelectron.* **2011**, *26*, 4559-4563.

(28) Liao, C. Z.; Mak, C. H.; Zhang, M.; Chan, H. L.; Yan, F. Flexible Organic Electrochemical Transistors for Highly Selective Enzyme Biosensors and Used for Saliva Testing. *Adv. Mater.* **2015**, *27*, 676-681.

(29) Mak, C. H.; Liao, C. Z.; Fu, Y.; Zhang, M.; Tang, C.Y.; Tsang, Y. H.; Chan, H. L.; Yan, F. Highly-Sensitive Epinephrine Sensors Based on Organic Electrochemical Transistors with Carbon Nanomaterial Modified Gate Electrodes. *J. Mater. Chem. C* **2015**, *3*, 6532-6538.

(30) Xiong, C.; Wang, Y.; Qu, H.; Zhang, L. J.; Qiu, L. Z.; Chen, W.; Yan, F.; Zheng, L. Highly Sensitive Detection of Gallic Acid Based on Organic Electrochemical Transistors with Poly(diallyldimethylammonium chloride) and Carbon nanomaterials Nanocomposites Functionalized Gate Electrodes. *Sens. Actuators B* **2017**, *246*, 235-242.

(31) Bihar, E.; Deng, Y. X.; Miyake, T.; Saadaoui, M.; Malliaras, G. G.; Rolandi, M. A Disposable Paper Breathalyzer with an Alcohol Sensing Organic Electrochemical Transistor. *Sci. Rep.* **2016**, *6*, 27582.

(32) Lin, P.; Luo, X. T.; Hsing, I-M.; Yan, F. Organic Electrochemical Transistors Integrated in Flexible Microfluidic Systems and Used for Label‐Free DNA Sensing. *Adv. Mater.* **2011**, *23*, 4035-4040.

(33) Fu, Y.; Wang, N. X.; Yang, A. N.; Law, H. K.; Li, L.; Yan, F. Highly Sensitive Detection of Protein Biomarkers with Organic Electrochemical Transistors. *Adv. Mater.* **2017**, *29*, 1703787.

(34) Kim, D. J.; Lee, N. E.; Park, J. S.; Park, I. J.; Kim, J. G.; Cho, H. J. Organic Electrochemical Transistor Based Immunosensor for Prostate Specific Antigen (PSA) Detection Using Gold Nanoparticles for Signal Amplification. *Biosens. Bioelectron.* **2010**, *25*, 2477-2482.

(35) He, R. X.; Zhang, M.; Tan, F.; Leung, P. H.; Zhao, X. Z.; Chan, H. L.; Yan, F. Detection of Bacteria with Organic Electrochemical Transistors. *J. Mater. Chem.* **2012**, *22*, 22072-22076.

(36) Lin, P.; Yan, F.; Yu, J. J.; Chan, H. L.; Yang, M. The Application of Organic Electrochemical Transistors in Cell‐based Biosensors. *Adv. Mater*. **2010**, *22*, 3655-3660.

(37) Frens, G. Controlled Nucleation for the Regulation of the Particle Size in Monodisperse Gold Suspensions. *Nature* **1973**, *241*, 20-22.

(38) Chen, Z. H.; Liu, Y.; Wang, Y. Z.; Zhao, X.; Li, J. H. Dynamic Evaluation of Cell Surface N-Glycan Expression via an Electrogenerated Chemiluminescence Biosensor Based on Concanavalin A-Integrating Gold-Nanoparticle-Modified $Ru(bpy)_3^{2+}$-Doped Silica Nanoprobe. *Anal. Chem*. **2013**, *85*, 4431-4438.

(39) Ge, S. G.; Lan, F. F.; Liang, L. L.; Ren, N.; Li, L.; Liu, H. Y.; Yu, J. H. Ultrasensitive Photoelectrochemical Biosensing of Cell Surface N-Glycan Expression Based on the Enhancement of Nanogold-Assembled Mesoporous Silica Amplified by Graphene Quantum Dots and Hybridization Chain Reaction. *ACS Appl. Mater. Interfaces* **2017**, *9*, 6670-6678.

(40) Fu, Y.; Liu, K.; Sun, Q. Q.; Lin, B.; Lu, D. Q.; Xu, Z. A.; Zhang, W. A Highly Sensitive Immunosensor for Calmodulin Assay Based on Enhanced Biocatalyzed Precipitation Adopting a Dual-Layered Enzyme Strategy. *Biosens. Bioelectron*. **2014**, *56*, 258-263.

(41) Hosokawa, N.; Wada, I.; Hasegawa, K.; Yorihuzi, T.; Tremblay, L. O.; Herscovics, A.; Nagata, K. A Novel ER α‐mannosidase-like Protein Accelerates ER‐associated Degradation. *EMBO Rep.* **2001**, *2*, 415-422.

(42) Liu, M.; Yu, X. C.; Chen, Z.; Yang, T.; Yang, D. D.; Liu, Q. Q.; Deng, Y. Aptamer Selection and Applications for Breast Cancer Diagnostics and Therapy. *J. Nanobiotechnol*. **2017**, *15*, 81.

(43) Mirkin, C. A.; Letsinger, R. L.; Mucic, R. C.; Storhoff, J. J. A DNA-based method for rationally assembling nanoparticles into macroscopic materials. *Nature*, **1996**, *382*, 607.

(44) Wang, D. G.; Xu, Z. A.; Yu, H. J.; Chen, X. Z.; Feng, B.; Cui, Z. R; Wang, J. Treatment of Metastatic Breast Cancer by Combination of Chemotherapy and Photothermal Ablation Using Doxorubicin-Loaded DNA Wrapped Gold Nanorods. *Biomaterials*, **2014**, *35*, 8374-8384.

(45) Guo, L. H.; Yang, X.; Ferhan, A. R.; Chen, G. N.; Kim, D. H. Oriented Gold Nanoparticle Aggregation for Colorimetric Sensors with Surprisingly High Analytical Figures of Merit. *J. Am. Chem. Soc.* **2013**, 135, 12338-12345.

(46) Aykul, S.; Martinez-Hackert, E. Determination of Half-Maximal Inhibitory Concentration Using Biosensor-Based Protein Interaction Analysis, *Anal. Biochem.* **2016**, 508, 97-103.

(47) Lin, P.; Yan, F.; Chan, H. L. Ion Sensitive Properties of Organic Electrochemical Transistors, *ACS Appl. Mater.Interfaces.* **2010**, 2, 1637-1641.

(48) Tang, H.; Yan, F.; Lin, P.; Xu, J. B.; Chan, H. L. Highly Sensitive Glucose Biosensors Based on Organic Electrochemical Transistors Using Platinum Gate Electrodes Modified with Enzyme and Nanomaterials. *Adv. Funct. Mater.* **2011**, 21, 2264–2272.

(49) Liao, C. Z.; Zhang, M.; Niu L. Y.; Zheng Z. J.; Yan, F. Highly selective and sensitive glucose sensors based on organic electrochemical transistors with graphene-modified gate electrodes, *J. Mater. Chem. B* **2013**, 1, 3820-3829.

(50) Yang, A.N.; Li, Y. Z.; Yang, C. X.; Fu, Y.; Wang, N. X.; Li, L.; Yan, F. Fabric Organic Electrochemical Transistors for Biosensors. *Adv. Mater*. **2018**. published online, doi: 10.1039/C7QM00497D.

Table of Content